Evidence for a large magnitude eruption from Campi Flegrei caldera (Italy) at 29 ka

Albert, PG.[1], Giaccio, B.[2], Isaia, R.[3], Costa, A.[4], Niespolo, EM.[5], Nomade, S.[6], Pereira, A.[6], Renne, PR.[5], Hinchliffe, A.[7], Mark, DF.[7], Brown, RJ.[8], Smith, VC.[1]

AFFILIATIONS

1. University of Oxford, RLAHA, Oxford, OX1 3TG, UK
2. Istituto di Geologia Ambientale e Geoingegneria, CNR, Roma, Italy
3. Istituto Nazionale di Geofisica e Vulcanologia, Osservatorio Vesuviano, Naples, Italy
4. Istituto Nazionale di Geofisica e Vulcanologia, Sezione di Bologna, Italy
5. Department of Earth and Planetary Science, University of California and Berkeley Geochronology Centre, Berkeley, USA
6. Laboratoire des Sciences du Climat et de l'Environnement (CEA-CNRS-UVSQ) and Université de Paris-Saclay Gif-Sur-Yvette, France
7. Scottish Universities Environmental Research Centre, East Kilbride, Scotland, G75 0QF, UK
8. Durham University, Department of Earth Sciences, Durham DH1 3LE, UK

ABSTRACT

The 40 ka caldera-forming eruption of Campi Flegrei (Italy) is the largest known eruption in Europe during the last 200 kyr, but little is known about other large eruptions at the volcano prior to a more recent caldera-forming event at 15 ka. At 29 ka a widespread volcanic ash layer, termed the Y-3 tephra, covered >150,000 km^2 of the Mediterranean. The glass compositions of the layer are consistent with Campi Flegrei being the source but no prominent proximal equivalent in the appropriate chrono-stratigraphic position had been previously identified. Here we report new glass chemistry data and $^{40}Ar/^{39}Ar$ ages (29.3 ± 0.7 ka [2σ]) that reveal the near-source Y-3 eruption deposit in a sequence at Ponti Rossi and a nearby borehole (S-19) in Naples. The dispersal and thickness of the deposits associated with this eruption, herein named the Masseria del Monte Tuff, were simulated using a tephra sedimentation model. The model indicates that ~16 km^3 DRE (dense rock equivalent) of the magma erupted was deposited as fall. This volume and the areal distribution suggest the Masseria del Monte Tuff was a magnitude 6.6 eruption (corresponding to VEI 6), similar to the 15 ka caldera-forming Neapolitan Yellow Tuff (M6.8) eruption at Campi Flegrei. However, the lack of coarse, thick, traceable, near-vent deposit suggests peculiar eruption dynamics. Our reconstruction and modelling of the eruption show the fundamental role that distal tephrostratigraphy can play in constraining the scale and tempo of past activity, especially at highly productive volcanoes.

INTRODUCTION

Near-vent volcanic successions often provide fragmentary records of past explosive volcanism due to the intense volcano-tectonic and syn-eruptive sedimentary processes they experience. This means they are not always representative of the full range in scale and tempo of past activity. Statistical analysis of existing eruptive databases verifies under-recording, including large magnitude eruptions (Kiyosugi et al., 2015), which is problematic for hazard assessments. Fortunately, explosive eruption deposits are recorded as ash (tephra) layers in sedimentary records. In the Mediterranean region the distal tephrostratigraphic record has been widely used as a key tool for studying past volcanism, reconstructing long-term eruption histories and constraining the tempo and dynamics of explosive eruptions (e.g., Paterne et al., 1988; Wulf et al., 2004).

Although some of the most widespread Mediterranean ash layers are correlated to near-source deposits, e.g., the Y-5 marine tephra linked to the Campanian Ignimbrite (CI) eruption of Campi Flegrei caldera (CFc) at 40 ka (e.g., Giaccio et al., 2017), many other widely dispersed tephra do not have counterparts near source. One of the most widespread layers not confidently correlated to a particular eruption deposit is the Y-3 tephra. This last-glacial tephra layer was first reported in the sediments of the Ionian Sea (Keller et al., 1978), and has been traced across the Mediterranean (**Fig. 1A; Table S1**). A precise age of 28,690-29,420 cal yrs BP was obtained for the Y-3 in the Tenaghi Philippon peat sequence, Greece (Albert et al., 2015). The glass compositions of the Y-3 tephra are consistent with CFc, but within the so-called 'Tufi Biancastri' (TB) succession (Orsi et al., 1996; Tomlinson et al., 2012) – encompassing all the eruption deposits between the ~15 ka Neapolitan Yellow Tuff (NYT; Deino et al., 2004) and CI (**Fig. 1B**). No deposit with the full range of compositions (phono-trachytic to trachytic) diagnostic of the distal layer had been found at source (see Albert et el., 2015). Here we report the characteristics of a mid-proximal TB deposit that correlates with the Y-3 distal layer, and helps verify the eruption was a large magnitude event.

PROXIMAL STRATIGRAPHY AND CHEMICAL COMPOSITIONS OF THE DEPOSITS

The distal Y-3 tephra has two volcanic glass compositional end-members, higher-SiO_2 trachytic (Component 1) and lower-SiO_2 phono-trachytic (Component 2) glasses, with the phono-trachytic glasses being particularly distinctive. Chemical analyses (methods see Data Repository 1) of TB units identified in a borehole (S-19) and an outcrop at Ponti Rossi (PR; **Fig. S1**), northeast of CFc in central Naples, show the two compositional end-members are consistent with the distal tephra (**Fig. 2; Table S2**).

The S-19 TB sequence is 14 meters thick with 6 primary tephra units that range from a few cm to 3.4 m in thickness. The thickest unit is the third above the CI, found at 25.90-22.50 m (3.40 m thick) and it presents the glass compositions of the distal Y-3 tephra (**Fig. 2**). The TB sequence at PR has eight eruption units separated by eruption hiatuses marked by soil formation (paleosols; Fig. 2). Similarly, the thickest unit in the TB succession at PR (90 cm), the fourth unit (CF131/132) above the CI, chemically corresponds to the distal Y-3 tephra (**Fig. 2; Fig. S2**).

The features of the S-19 drill core (25.9-22.50 m) and PR (CF131-132) units are similar. Both are characterised by a lower sub-unit of fall containing a bed of moderately sorted pumice lapilli (5-10 cm thick), and an upper sub-unit (up to 3.30 m thick in S-19) of poorly-sorted ash-dominated pyroclastic density current (PDC) deposits. The PDC sub-unit contains abundant, distinctively large (up to 3 cm diameter) accretionary lapilli which are exclusive to these TB units. The main difference between the two localities is the thickness; the PDC sub-unit of S-19 is considerably thicker than at PR (50cm), either reflecting paleotopography or post-depositional erosion. Detailed descriptions of the S-19/PR tephra successions are provided in Data Repository 1.

The compositional glass data for the PR (samples CF131 and CF132) and S-19 (samples 25.8m and 22.9m) units verify their lithostratigraphic correlation. They are the only TB eruption deposits to contain three compositional groupings (**Fig. 2A**). The Component 1 glasses are high-SiO_2 (~61.6-62.4 wt.%) trachytic glasses with ~8.3-8.7 wt.% K_2O (**Fig. 2A**), they are enriched in incompatible trace elements (e.g., ~30-33 ppm Th), and match the trachytic end-member of the distal Y-3 (**Fig. 2**). Component 2 glasses are lower in SiO_2 (~59.8-60.6 wt.%), have higher K_2O contents (~9.7-10.3 wt.%; **Fig. 2**), and lower levels incompatible trace element enrichment (e.g., ~14-15 ppm Th) - consistent with the distinctive phono-trachytic end-member of the Y-3 tephra **(Fig. 2)**.

The third, less abundant and more chemical variable component, are lower SiO_2 trachytic glasses (~57.6-60.8 wt.%) and show the lowest K_2O contents (~7.9-8.3 wt.%; **Fig. 2**) observed in the investigated deposits.. The Component 3 glasses are not observed in the upper portion of the thicker S-19 borehole (25.8-22.50 m) unit, or the widespread Y-3 tephra, this implies the widespread ash dispersal is not associated with the earliest phase of the eruption.

$^{40}Ar/^{39}Ar$ GEOCHRONOLOGY

Sanidine crystals from three near-source pyroclastic samples stratigraphically and chemically related to the distal Y-3 were dated using $^{40}Ar/^{39}Ar$ methods at the Laboratoire des Science du Climat et de l'Environment (LSCE), France (sample 22.9m - top of the S-19 borehole unit) and at the Berkeley Geochronology Centre (BGC), USA (sample 25.8m - base of the S-19 unit; sample CF132 upper portion of the PR unit). Weighted mean ages are calibrated to the age of the Alder Creek Sanidine (ACs) =1.1891 ± 0.0008 Ma (1σ, Niespolo et al., 2017) and calculated using the decay constants of Renne et al. (2011). Analytical methods and instrumentation used are fully outlined in the Data Repository 1, along with probability diagrams (**Fig. S3-7**), and *R*-values (**Table S3**). The $^{40}Ar/^{39}Ar$ weighted mean ages are presented in a summary age probability diagram at 2σ uncertainty (**Fig. 3**).

The ages of individual crystals analysed from the S-19 22.9 m sample show a bimodal distribution with a dominant younger population (~29 ka) and an older population at ~40 ka (**Fig. 3**). The $^{40}Ar/^{39}Ar$ weighted mean age determined for this upper portion of the eruption deposit is 29.0 ± 0.8 ka [2σ] (MSWD=0.4, P=1, *n*=18). The older crystals cluster about the age of the CI eruption (40 ka) and are considered xenocrysts from parts of the crystallised magmatic system or deposits of the CI. The whole 2 sigma age range of the CI xenocrysts identified in the S-19 22.9 m sample are used, in conjunction with the stratigraphic position of all correlated samples above the CI, as a basis to exclude CI xenocrysts from the remaining analyses.

The exclusion of CI xenocrysts produces a $^{40}Ar/^{39}Ar$ weighted mean age of 28.4 ± 2.1 (MSWD=0.52, P=1, *n*=44) for the 25.8m basal sample of the borehole unit. The combined $^{40}Ar/^{39}Ar$ weighted mean age for the S-19 25.9-22.5m (samples 25.8m and 22.9m) eruption deposit is 29.0 ± 0.8 ka. The CI xenocrysts excluded $^{40}Ar/^{39}Ar$ age determinations for the PR deposit (sample CF132), are 31.6 ± 2.8 (MSWD=0.33, P=1, *n*=23) using Nexus, and 31.3 ± 2.6 (MSWD=0.15, P=1, *n*=44) from Noblesse, these ages are statistically indistinguishable from one another. The combined $^{40}Ar/^{39}Ar$ weighted mean age for the PR eruption deposit (CF131/132) is 31.4 ± 1.9 ka.

The S-19 and PR $^{40}Ar/^{39}Ar$ ages are statistically indistinguishable at the 95.4% confidence level and can be combined to provide a $^{40}Ar/^{39}Ar$ weighted mean age of 29.3 ± 0.7 ka

(MSWD=0.5, P=1, *n*=96) for the eruption deposit, which perfectly overlap with radiocarbon age determinations for the distal Y-3 tephra (**Fig. 3**), verifying the stratigraphic and chemical correlations.

ASSESSING THE ASH DISPERSAL AND PDC VOLUMES

The ash dispersal was simulated using a semi-analytical dispersal model HAZMAP (Macedonio et al., 2005). Integrating near-source and distal (Y-3) tephra fall deposit thicknesses (**Table S1**) within a HAZMAP model allows us to constrain the eruption parameters (**Table S4**; Costa et al., 2009). Some reported Y-3 localities could not be used because either layer thicknesses are not reported, or they are likely inflated due to the depositional setting (e.g. marine canyons).

The modelled dispersal pattern for the Y-3 tephra **(Fig. 1A)** reproduced the recorded thicknesses within an order of magnitude, with all but one of the modelled thickness values being between 1/3 and 3 times the observed thickness at each locality (**Fig. S8**). The limitations of this modelling approach are outlined in Matthews et al. (2012), and the uncertainties are large due to the lack of data and assumptions (e.g. deposit density does not change over the area, assumed bulk granulometry). However, these results place constraints on the order of magnitude of the eruption, revealing that the fall comprised ~16 km^3 DRE (assuming a rock density of 2350 kg/m^3) of ejected magma, from a column that reached ~59 km high. The volume of the near-source PDC was estimated at a minimum of ~1 km^3 DRE using the Delaunay Triangulation method of Macedonio and Pareschi, (1991), which is suitable for reconstructing the volume of geological horizons where the thickness values are irregularly-spaced (**Table S1**). Combining the HAZMAP fall volume with that of the PDC indicates that the total volume of the eruption would be ~17 km^3 DRE, which equates to a VEI 6 (after Newhall and Self, 1982) or at least a magnitude 6 eruption (M6.6, following Pyle, 2000).

THE MASSERIA DEL MONTE TUFF ERUPTION DYNAMICS AND HAZARDS AT CFc

The modelled eruption parameters (**Table S4**) would imply that the herein named Masseria del Monte Tuff (named after the most proximal TB succession), responsible for the Y-3 tephra, is similar in magnitude and more widely dispersed as a visible fall deposit than the younger NYT **(Fig.1A)** caldera-forming eruption (recalculated to ~25 km^3 DRE; following Deino et al., 2004) of CFc. Given the amount of magma erupted during the Masseria del Monte Tuff it is likely to have generated a caldera. The lack of physical evidence implies that if one was generated, it must have been within the collapse structure of the younger NYT.

Although the Masseria del Monte Tuff and NYT eruptions were a similar order of magnitude, there is a stark contrast between their PDC deposits. At similar distances from the caldera wall, the PDC deposits of the eruption are thin (~ 3.3 m) relative to the ~16 m thick deposits of the NYT. Consequently, it seems likely that the eruption mechanisms of these two large magnitude events were very different; however, due to the limited near-source exposures of the Masseria del Monte Tuff we must use the distal ash fall and ash dispersal modelling to gain a better understanding of the eruption mechanisms.

Given the estimated magnitude of the eruption, the area covered by the Y-3 tephra is somewhat restricted, illustrated by its absence in the eastern Mediterranean marine records (**Fig. 1**), this suggests efficient aggregation of fine ash. This premature fallout of the finest material, coupled with the high density of the aggregates (modelled to be 1000 kg/m^3) and the presence of large accretionary lapilli in proximal outcrops is consistent with the presence of liquid water in the plume (Mastin et al., 2016). The modelled column height and the effective diffusion (accounting for the effects of both atmosphere and volcanic plume turbulence) of ~7x10^4 m^2/s both imply a large mass flow rate (Costa et al., 2013; 2018), which is consistent with a co-ignimbrite plume in the incipient collapsing regime (estimated between 10^9 and 10^{10} kg/s by Costa et al., 2018). These plumes are transitional between a Plinian and co-ignimbrite column and can extend up to 60 km (cf. Costa et al., 2018). The modelled results are consistent with the lack of a prominent coarse-grain deposit close to the vent, which suggest an unstable eruption column intermittently generating PDCs. The absence of one of the glass populations in the upper portion of the near-source deposits and in the distal Y-3 implies that the widely dispersed ash was largely associated with a co-ignimbrite plume generated by late PDC phase/s. Similarly, the co-ignimbrite plume significantly contributed to the enormous CI ash dispersal across the eastern Mediterranean (Smith et al., 2016). From a hazard perspective, recognition of a large magnitude eruption between the CI (40 ka) and NYT (15 ka) eruptions, drastically reduces the reoccurrence interval of large magnitude events at CFc. With the Masseria del Monte eruption dated at 29 ka, the time elapsed between large magnitude eruptions (≥M6/VEI 6) at this densely populated volcano is halved to ~12.5 kyr.

CONCLUSIONS

The Masseria del Monte Tuff erupted at CFc is dated at 29.3 ± 0.7 ka [2σ] and was a large magnitude (M6.6 or VEI 6) event that erupted around ~17 km^3 (DRE) of magma based largely on the distal ash fall covering an area >150,000 km^2. Reconstructed eruption parameters using the HAZMAP model suggest the deposits are consistent with dispersal from a co-ignimbrite plume in the incipient collapsing regime. The recognition of such a large-magnitude event, only 29 ka ago, illustrates that the near-source record of volcanism at one of the most productive volcanoes in Europe is not fully representative. It also highlights that by integrating distal and near-source records and using ash dispersal models it is possible to better constrain the magnitude, eruptive mechanisms and tempo of volcanism. This is particularly pertinent at volcanoes that commonly experience caldera collapse and the deposition of thick pyroclastic successions, which make the record of past activity hard to access.

ACKNOWLEDGEMENTS

PGA and VCS acknowledge funding from Leverhulme (ECF-2014-438) and the John Fell Fund. PRR and EMN thank the Ann and Gordon Getty Foundation and Chihiro Ishida for sample preparation assistance. AC and RI acknowledge the MIUR project Premiale Ash-RESILIENCE Dr. Emma Tomlinson and John Pouncett are thanked for assistance with the trace element analysis, and cartography, respectively. We thank Martine Paterne, Jenni Barclay and a anonymous Reviewer for their constructive comments.

REFERENCES CITED

Albert, P.G., Hardiman, M., Keller, J, Tomlinson, E.L., Bourne, A, J., Smith, V.C. Wulf, S., Zanchetta, G., Sulpizio, R., Müller, U.C., Pross, J., Ottolini, L., Matthews, I.P., Blockley, S.P., Menzies, M.A., 2015, The Y-3 tephrostratigraphic marker revisited: new diagnostic glass geochemistry, improved chronology and climatostratigraphic interpretations: *Quat. Sci. Rev* 118, 105-121.

Costa, A., Suzuki, Y.J., Koyaguchi, T., 2018, Understanding the plume dynamics of explosive super-eruptions: *Nat. Commun.* DOI: 10.1038/s41467-018-02901-0

Costa, A., Dell'Erba, F., Di Vito, M.A., Isaia, R., Macedonio, G., Orsi, G., Pfeiffer, T., 2009, Tephra fallout hazard assessment at the Campi Flegrei caldera (Italy): *Bull. Volcanol.* 71(3), 259-273.

Deino, A.L., Orsi, G., de Vita, S., Piochi, M., 2004, The age of the Neapolitan Yellow Tuff caldera-forming eruption (Campi Flegrei caldera – Italy) assessed by ^{40}Ar/^{39}Ar dating method: *J. Volcanol. Geotherm. Res.* 133 (1–4), 157-170.

Giaccio, B., Hajdas, I., Isaia, R., Deino, A., Nomade, S., 2017, High-precision ^{14}C dating and ^{40}Ar/^{39}Ar dating of the Campanian Ignimbrite (Y-5) reconciles the time-scales of climatic-cultural processes at 40 ka: *Sci. Rep*. 7, 45940.

Keller, J., Ryan, W.B.F., Ninkovich, D., Altherr, R., 1978, Explosive volcanic activity in the Mediterranean over the past 200,000 yrs as recorded in deep-sea sediments: *Geol Soc Am Bull* 89, 591–604.

Kiyosugi, K., Connor, C., Sparks, R.S.J., Crosweller, H.S., Brown, S.K., Siebert, L., Wang, T., Takarada, S., 2015, How many explosive eruptions are missing from the geological record? Analysis of the Quaternary record of large magnitude explosive eruptions in Japan: *J. Appl. Volcanol*. 4:17.

Macedonio, G., Costa, A., Longo, A., 2005, A computer model for volcanic ash fallout and assessment of subsequent hazard: *Comput. Geosci*. 31, 837-845.

Macedonio, G. and Pareschi, M.T., 1991, An algorithm for the triangulation of arbitrarily distributed points: Applications to volume estimates and terrain fitting: *Comput. Geosci.* 17, 859-874.

Mastin, L.G., Van Eaton, A.R., Durant, A.J., 2016, Adjusting particle-size distributions to account for aggregation in tephra-deposit model forecasts: *Atmos. Chem. Phys*., 16, 9399–9420.

Matthews, N.E., Smith, V.C., Costa, A., Durant, A.J., Pyle, D.M., Pearce, N.J.G., 2012, Ultra-distal tephra deposits from super-eruptions: Examples from Toba, Indonesia and Taupo Volcanic Zone, New Zealand: *Quat. Int.* 258, 54-79.

Newhall, C.G., Self, S., 1982. The Volcanic Explosivity Index (VEI) e an estimate of the explosive magnitude for historical volcanism. Journal of Geophysical Research 87 (C2), 1231-1238.

Niespolo, E.M., Rutte, D., Deino, A.L., Renne, P.R., 2017, Intercalibration and Age of the Alder Creek ^{40}Ar/^{39}Ar standard: *Quat. Geochronol*. 39, 205-213.

Orsi, G., DeVita, S., Di Vito., 1996. The restless, resurgent, Campi Flegrei nested caldera (Italy): Constraints on its evolution and configuration: *J. Volcanol. Geotherm. Res.* 74(3-4), 179-214.

Paterne, M., Guichard, F., Labeyrie, J. 1988, Explosive activity of the South Italian volcanoes during the past 80,000 years as determined by marine tephrochronology: *J. Volcanol. Geotherm. Res.* 34, 153-172.

Pyle, D.M., 2000, Sizes of volcanic eruptions. In Encyclopedia of Volcanoes: Edited by: Sigurdsson H, Houghton BF, McNutt SR, Rymer H, Stix J: Academic Press, London; 2000.

Ramsey, C. B., Albert, P.G., Blockley, S., Hardiman, M., Housley, R., Lane, C.S., Lee, S., Matthews, I.P., Smith, V.C., Lowe, J., 2015. Improved age estimates for key Late Quaternary European tephra horizons in the RESET lattice: *Quat. Sci. Rev.*118, 18-32.

Renne, P.R., Balco, G., Ludwig, K.R., Mundil, R., Min, K., 2011, Response to the comment by W.H. Schwarz et al. on "Joint determination of ^{40}K decay constants and ^{40}Ar*/^{40}K for the Fish Canyon sanidine standard, and improved accuracy for ^{40}Ar/^{39}Ar geochronology" by PR Renne, et al. (2010): *Geochim. Cosmochim. Acta* 75, 5097-5100.

Smith, V.C., Isaia, R., Engwell, S., Albert, P.G., 2016, Tephra dispersal during the Campanian Ignimbrite (Italy) eruption: implications for ultra-distal ash transport during the large caldera-forming eruption: *Bull. Volcanol.* 78:45.

Smith, V.C., Isaia, R., Pearce, N.J.G., 2011, Tephrostratigraphy and glass compositions of post-15 kyr Campi Flegrei eruptions: implications for eruption history and chronostratigraphic markers: *Quat. Sci. Rev.* 30, 3638-3660.

Tomlinson, E.L, Arienzo, I., Civetta, L., Wulf, S., Smith, V.C., Hardiman, M., Lane, C.S., Carandente, A., Orsi, G., Rosi, M., Muller, W., Thirwall, M.F., Menzies, M., 2012, Geochemistry of the Phlegraean Fields (Italy) proximal sources for major Mediterranean tephras: implications for the dispersal of Plinian and co-ignimbritic components of explosive eruptions: *Geochim. Cosmochim. Acta* 93, 102-128

Wulf, S., Kraml, M., Brauer, A., Keller, J., Negendank, J.F.W., 2004, Tephrochronology of the 100 ka lacustrine sediment record of Lago Grande di Monticchio (southern Italy): *Quat. Int.* 122, 7–30.

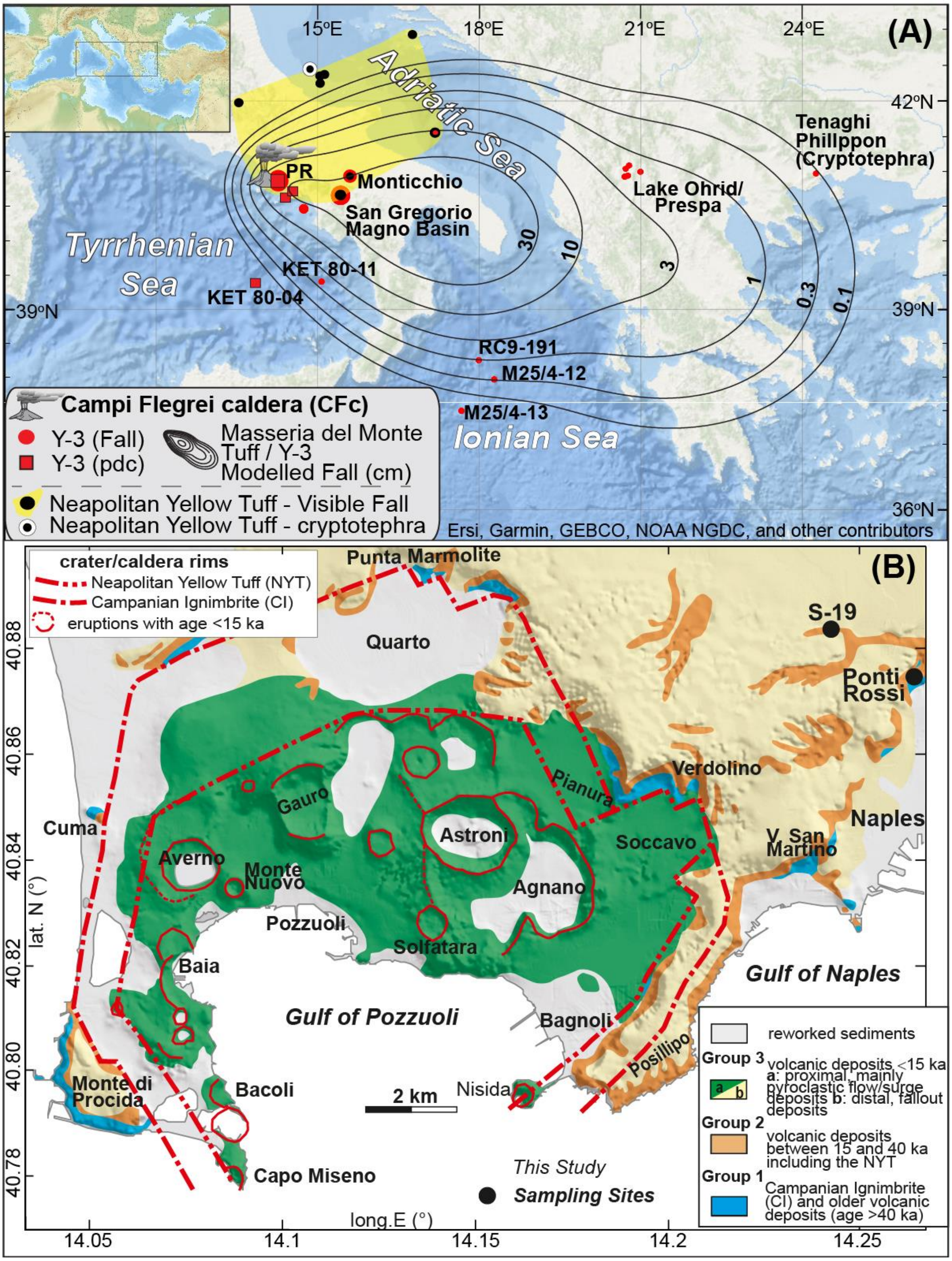

Figure 1: (A) The distribution of Y-3 tephra occurrences across the central Mediterranean (**Table S1**), and for comparison the Neapolitan Yellow Tuff(NYT). Overlain is the HAZMAP isopach map of the Masseria del Monte Tuff linked to the Y-3 tephra. (B) A map of Campi Flegrei caldera (CFc) and it major structures, and sampling localities are shown.

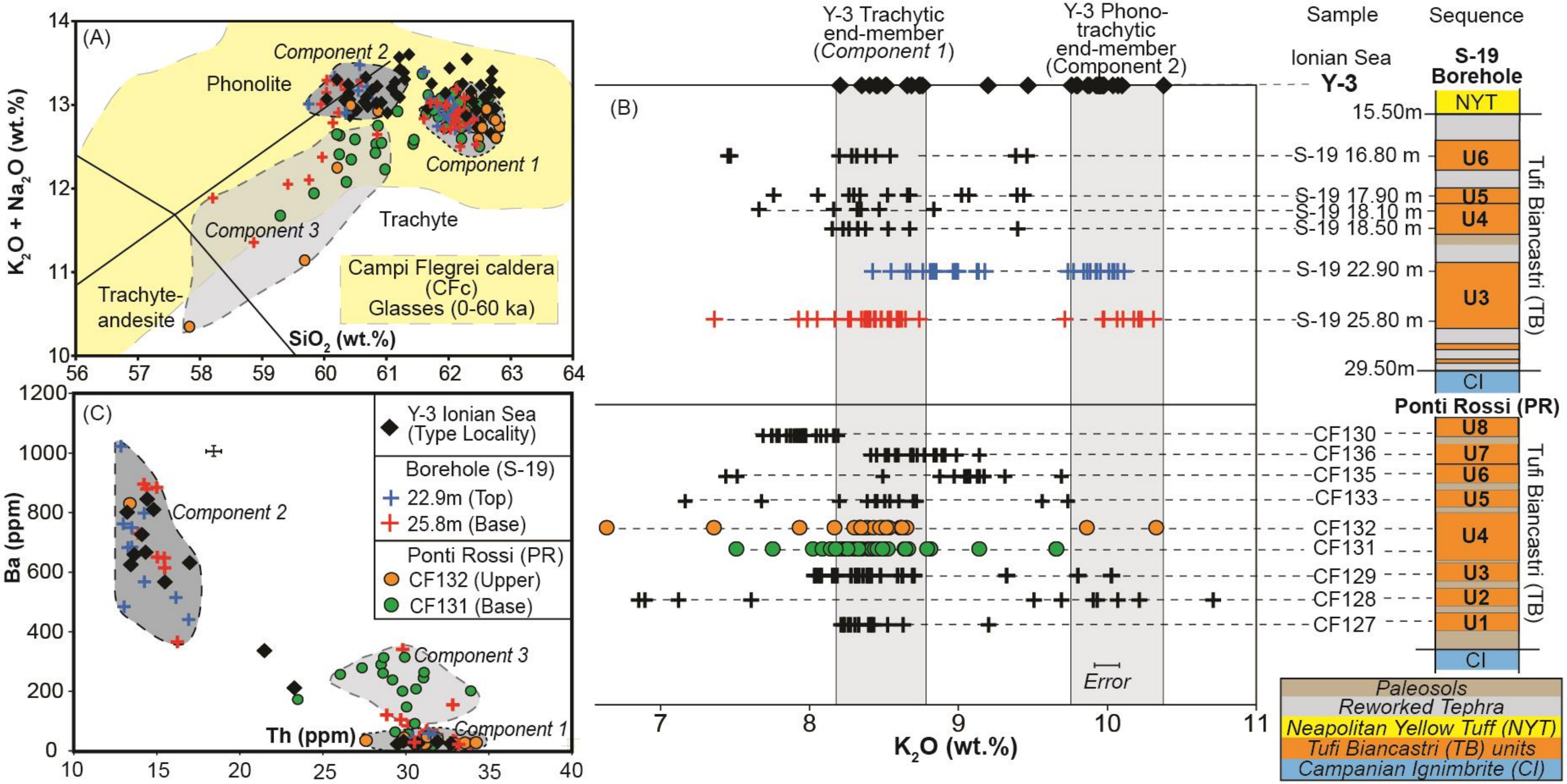

Figure 2: (A) The distal Y-3 tephra has two dominant components, a trachytic (Component 1) and phono-trachytic (Component 2) end-member, both consistent with CFc glasses (Smith et al., 2011; Tomlinson et al., 2012). The TB units related here to the distal Y-3 at Ponti Rossi (PR) (CF131/132) and in the S-19 Borehole (25.9-22.5m) have the same two components, plus a population of lower SiO_2 trachytes (Component 3). **(B)** The two end-members of the distal Y-3 are distinguished using their K_2O content of their volcanic glasses (*grey boxes*), only the third unit in borehole S-19, and the third (CF129) and forth unit (CF131-132) in the PR sequence have both component 1 and 2 compositions. The thin ash unit (3; CF129) underlying Unit 4 at PR is inconsistent with the Y-3 tephra based on its levels of trace element enrichment (**Fig. S1E-F**). **(C)** Trace elements analysis verifies that both end-members of the Y-3 (Component 1 and 2) are observed in the thickest near-source units at PR and in the S-19 borehole.

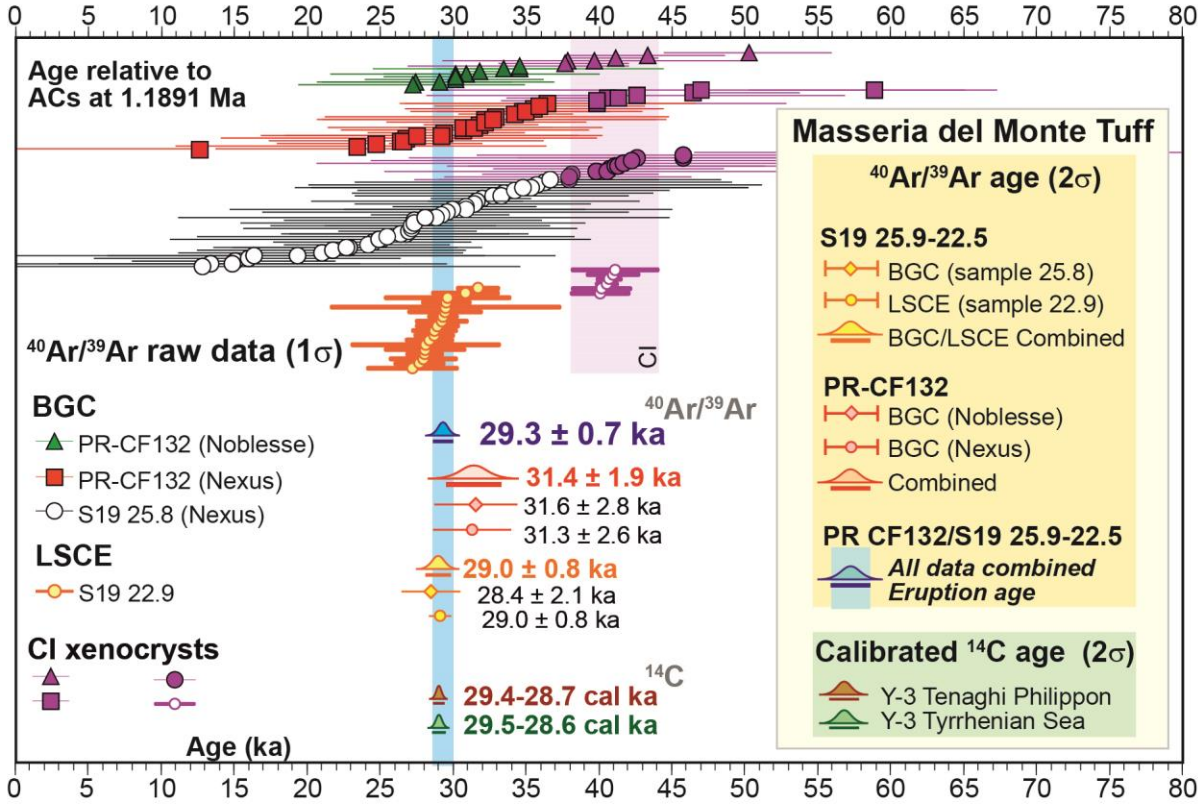

Figure 3: $^{40}Ar/^{39}Ar$ ages (2σ) of proximal CFc samples of the Masseria del Monte Tuff, and terrestrial (Albert et al., 2015) and marine (Ramsey et al., 2015) ^{14}C ages of the distal Y-3. Individual sanidine age determinations are shown with 1σ errors and xenocrysts (mostly 40 ka CI crystals) are removed from all age calculations.